

**REPORT NO.
UCB/SEMM 89/17**

**STRUCTURAL ENGINEERING,
MECHANICS AND MATERIALS**

**A ROBUST QUADRILATERAL MEMBRANE FINITE
ELEMENT WITH DRILLING DEGREES OF FREEDOM**

By:

A. IBRAHIMBEGOVIC, R.L. TAYLOR and E.L. WILSON

AUGUST 1989

**DEPARTMENT OF CIVIL ENGINEERING
UNIVERSITY OF CALIFORNIA
BERKELEY, CALIFORNIA**

A Robust Quadrilateral Membrane Finite Element with Drilling Degrees of Freedom

Adnan Ibrahimbegovic[†], Robert L. Taylor[‡] and Edward L. Wilson[‡]

Department of Civil Engineering

University of California, Berkeley, CA 94720, U.S.A.

Abstract

A quadrilateral membrane finite element with drilling degrees of freedom is derived from variational principles employing independent rotation field. Both displacement based and mixed approach are investigated. The element exhibits excellent accuracy characteristics. When combined with a plate bending element, the element provides an efficient tool for linear analysis of shells.

Contents

1. Introduction
2. Variational Formulation
3. Finite Element Interpolation
4. Numerical Evaluation
5. Closure
6. References

[†] Assistant Research Engineer

[‡] Professor

A Robust Quadrilateral Membrane Finite Element with Drilling Degrees of Freedom

Adnan Ibrahimbegovic[†], Robert L. Taylor[‡] and Edward L. Wilson[‡]

Department of Civil Engineering

University of California, Berkeley, CA 94720, U.S.A.

1. Introduction

The need for membrane elements with drilling degrees of freedom (see Figure 1) arises in many practical engineering problems (e.g. in-filled frames, folded plates etc.). When combined with a bending element, a membrane element of this kind provides a versatile tool for analysis of shells. While early efforts to construct an element of this type were unsuccessful, more recent works, including the independent approaches of Allman[1984] and Bergan&Fellipa [1985], opened the perspectives for a successful solution. As a result, the revived interest of engineering community in membrane elements with drilling degrees of freedom is manifested by a series of papers on the subject (e.g. Taylor&Simo [1985], Carpenter et al. [1985], Allman [1987], Taylor [1987], Allman [1988], MacNeal&Harder [1988]). However, most of the proposed solutions are based on some form of 'free formulation', which concentrates solely on the choice of the finite element interpolation fields. The clever procedures of the finite element 'technology' are used to improve the performance of proposed elements.

[†] Assistant Research Engineer

[‡] Professor

A novel approach, which relies on a variational formulation employing an independent rotation field, has been presented recently by Hughes&Brezzi [1989]. Reissner [1965] was the first to suggest a variational formulation which utilized the skew-symmetric part of the stress tensor as a Lagrange multiplier to enforce the equality of independent rotations with the skew-symmetric part of the displacement gradient. However, in a significant contribution to the solution of this problem, Hughes&Brezzi [1989] have extended Reissner's formulation by recognizing instability of discrete approximations and suggested a way in which the discrete approximation can be stabilized. Some membrane elements with drilling degrees of freedom, derived from the displacement-type formulation of Hughes&Brezzi, are presented by Hughes et al. [1989]. Their work has assumed that the variational formulation employs an independent rotation field, i.e. strictly speaking it is based on the separate kinematics variables, of displacement and rotation.

In this work, we extend the applications of the Hughes&Brezzi to combine an Allman-type interpolation for the displacement field combined with an independently interpolated rotation field. A mixed-type variational formulation is presented with the skew-symmetric part of the stress tensor introduced as a Lagrange multiplier to enforce the equality of independent rotations with the skew-symmetric components of displacement gradient. A penalty displacement-type formulation with selective reduced integration is also employed. The displacement and rotation fields are the same in both formulations. In the mixed-type formulation the skew-symmetric part of stress is chosen constant over each element.

An outline of the paper is as follows. In Section 2 we give a short review for both the displacement-type and the mixed-type variational formulation. Our consideration follows closely the work of Hughes&Brezzi [1989]. The finite element interpolation and the discrete versions for both variational formulations is given in Section 3. Numerical evaluations of the derived membrane elements are presented in Section 4. Some closing remarks are given in Section 5.

2. Variational Formulation

In this section we follow closely the work of Hughes&Brezzi [1989]. The same index-free notation is utilized. For the sake of brevity, the discussion of boundary conditions is omitted. Inclusion of boundary conditions presents no difficulties for considerations to follow, and it can be handled in a standard manner (e.g., see Hughes [1987]). We also limit ourselves to linear elastostatic problems.

Let Ω be a region occupied by a body. The boundary value problem under consideration is: For all $\mathbf{x} \in \Omega$

$$\text{div } \boldsymbol{\sigma} + \mathbf{f} = \mathbf{0} \quad (2.1)$$

$$\text{skew } \boldsymbol{\sigma} = \mathbf{0} \quad (2.2)$$

$$\boldsymbol{\psi} = \text{skew } \nabla \mathbf{u} \quad (2.3)$$

$$\text{symm } \boldsymbol{\sigma} = \mathbf{C} \cdot \text{symm } \nabla \mathbf{u} \quad (2.4)$$

where (2.1) to (2.4) are, respectively, the equilibrium equations, the symmetry conditions for stress, the definition of rotation in terms of displacement gradient, and the constitutive equations.

In (2.1) to (2.4) the Euclidian decomposition of second-rank tensors is employed, e.g.

$$\boldsymbol{\sigma} = \text{symm } \boldsymbol{\sigma} + \text{skew } \boldsymbol{\sigma} \quad (2.5)$$

where

$$\text{symm } \boldsymbol{\sigma} = \frac{1}{2} (\boldsymbol{\sigma} + \boldsymbol{\sigma}^T) \quad (2.6)$$

$$\text{skew } \boldsymbol{\sigma} = \frac{1}{2} (\boldsymbol{\sigma} - \boldsymbol{\sigma}^T) \quad (2.7)$$

For the isotropic case and plane stress state, the constitutive modulus tensor $\mathbf{C} = \{C_{ijkl}\}$ has the form

$$C_{ijkl} = \lambda \delta_{ij} \delta_{kl} + \mu (\delta_{ik} \delta_{jl} + \delta_{il} \delta_{jk}) \quad i, j, k, l \in \left\{ 1, 2 \right\} \quad (2.8)$$

where

$$\lambda = \frac{\nu E}{(1-\nu^2)} \quad (2.9)$$

$$\mu = \frac{E}{2(1+\nu)} \quad (2.10)$$

while E and ν are Young's modulus and Poisson's ratio, respectively.

Reissner [1965] presented a variational formulation for the boundary value problem (2.1) to (2.4). This principle leads to a formulation which is inappropriate for numerical applications. Essentially, too many parameters for the skew-symmetric part of σ exist and the numerical problem fails the *LBB* conditions as well as the counts for the mixed patch test (e.g., see Zienkiewicz&Taylor [1989]). Hughes and Brezzi modified variational problem of Reissner in order to preserve the stability of the discrete problem. The modification (see Hughes&Brezzi [1989]) preserves (2.1) to (2.4) as the Euler-Lagrange equations. In addition, the symmetrical components of stress are eliminated using the constitutive equations (2.4) to give

Problem (M)

$$\begin{aligned} \Pi_\gamma(\mathbf{v}, \boldsymbol{\omega}, \text{skew } \boldsymbol{\tau}) &= \frac{1}{2} \int_{\Omega} \text{symm } (\nabla \mathbf{v}) \cdot \mathbf{C} \cdot (\text{symm } \nabla \mathbf{v}) \, d\Omega + \int_{\Omega} \text{skew } \boldsymbol{\tau}^T \cdot (\text{skew } \nabla \mathbf{v} - \boldsymbol{\omega}) \, d\Omega \\ &\quad - \frac{1}{2} \gamma^{-1} \int_{\Omega} |\text{skew } \boldsymbol{\tau}|^2 \, d\Omega - \int_{\Omega} \mathbf{v} \cdot \mathbf{f} \, d\Omega \end{aligned} \quad (2.11)$$

where $\mathbf{v} \in \mathbf{V}$, $\boldsymbol{\omega} \in \mathbf{W}$, $\boldsymbol{\tau} \in \mathbf{T}$ are spaces of trial displacements, rotations and stresses. This variational formulation requires that the rotations $\boldsymbol{\omega}$ and stresses $\boldsymbol{\tau}$ together with both the displacement \mathbf{v} and displacement derivatives, belong to the space of square-integrable functions over the region Ω .

The variational equation which results from variations on (2.11)

$$\begin{aligned} 0 &= D\Pi_\gamma(\mathbf{u}, \boldsymbol{\psi}, \text{skew } \boldsymbol{\sigma}) \cdot (\mathbf{v}, \boldsymbol{\omega}, \text{skew } \boldsymbol{\tau}) = \int_{\Omega} (\text{symm } \nabla \mathbf{v}) \cdot \mathbf{C} \cdot (\text{symm } \nabla \mathbf{u}) \, d\Omega \\ &\quad + \int_{\Omega} \text{skew } \boldsymbol{\tau}^T \cdot (\text{skew } \nabla \mathbf{u} - \boldsymbol{\psi}) \, d\Omega + \int_{\Omega} (\text{skew } \nabla \mathbf{v}^T \cdot \text{skew } \boldsymbol{\sigma} - \boldsymbol{\omega}^T \cdot \text{skew } \boldsymbol{\sigma}) \, d\Omega \end{aligned}$$

$$- \gamma^{-1} \int_{\Omega} \text{skew } \boldsymbol{\tau}^T \cdot \text{skew } \boldsymbol{\sigma} \, d\Omega - \int_{\Omega} \mathbf{v} \cdot \mathbf{f} \, d\Omega \quad (2.12)$$

In the next section the variational equation (2.12) is used to construct a mixed-type discrete formulation. It is possible to eliminate the skew-symmetric part of the stress tensor (see Hughes&Brezzi [1989]) by substituting

$$\gamma^{-1} \text{skew } \boldsymbol{\sigma} = \text{skew } \nabla \mathbf{u} - \boldsymbol{\psi} \quad (2.13)$$

into *Problem (M)* to obtain

Problem (D)

$$\begin{aligned} \tilde{\Pi}_{\gamma}(\mathbf{v}, \boldsymbol{\omega}) &= \frac{1}{2} \int_{\Omega} \text{symm } (\nabla \mathbf{v}) \cdot \mathbf{C} \cdot (\text{symm } \nabla \mathbf{v}) \, d\Omega \\ &+ \frac{1}{2} \gamma \int_{\Omega} |\text{skew } \nabla \mathbf{v} - \boldsymbol{\omega}|^2 \, d\Omega - \int_{\Omega} \mathbf{v} \cdot \mathbf{f} \, d\Omega \end{aligned} \quad (2.14)$$

The corresponding variational equation now is

$$\begin{aligned} 0 &= D \tilde{\Pi}_{\gamma}(\mathbf{u}, \boldsymbol{\psi}) \cdot (\mathbf{v}, \boldsymbol{\omega}) = \int_{\Omega} (\text{symm } \nabla \mathbf{v}) \cdot \mathbf{C} \cdot (\text{symm } \nabla \mathbf{u}) \, d\Omega \\ &+ \gamma \int_{\Omega} (\text{skew } \nabla \mathbf{v} - \boldsymbol{\omega})^T \cdot (\text{skew } \nabla \mathbf{u} - \boldsymbol{\psi}) \, d\Omega - \int_{\Omega} \mathbf{v} \cdot \mathbf{f} \, d\Omega \end{aligned} \quad (2.15)$$

The variational equation (2.15) is taken as the basis for constructing displacement-type discrete formulation which is presented in the next section.

The parameter γ , which appears in the formulations is problem dependent (see Hughes&Brezzi [1989]). For isotropic elasticity and Dirichlet boundary value problem Hughes et al. [1989] suggest γ be taken as shear modulus value, i.e. $\gamma = \mu$. However, the numerical studies we have performed, have shown that the formulation is insensitive to the value of γ used (at least for several orders of magnitude which bound the shear modulus).

3. Finite Element Interpolation

The particular choice for finite dimensional spaces $\mathbf{V}^h, \mathbf{W}^h, \mathbf{T}^h$ (subspaces of $\mathbf{V}, \mathbf{W}, \mathbf{T}$, respectively) is presented in this section along with the resulting discrete formulations.

We first consider the discrete version of *Problem (M)*

Problem (M^h)

$$\begin{aligned}
0 = & \int_{\Omega^e} (\text{symm } \nabla \mathbf{v}^h) \cdot \mathbf{C} \cdot (\text{symm } \nabla \mathbf{u}^h) d\Omega + \int_{\Omega^e} \text{skew } \boldsymbol{\tau}^{hT} \cdot (\text{skew } \nabla \mathbf{u}^h - \boldsymbol{\psi}^h) d\Omega \\
& + \int_{\Omega^e} (\text{skew } \nabla \mathbf{v}^{hT} \cdot \text{skew } \boldsymbol{\sigma}^h - \boldsymbol{\omega}^{hT} \cdot \text{skew } \boldsymbol{\sigma}^T) d\Omega \\
& - \gamma^{-1} \int_{\Omega^e} \text{skew } \boldsymbol{\tau}^{hT} \cdot \text{skew } \boldsymbol{\sigma}^h d\Omega - \int_{\Omega^e} \mathbf{v}^h \cdot \mathbf{f} d\Omega
\end{aligned} \quad (3.1)$$

We consider a 4-node quadrilateral element with degrees of freedom shown in Figure 1. The independent rotation field is interpolated as a standard bilinear field over each element. Accordingly

$$\mathbf{u}_3 \equiv \boldsymbol{\psi}^h = \sum_e \sum_{I=1}^4 N_I^e(r,s) \boldsymbol{\psi}_I \quad (3.2)$$

where (e.g., see Zienkiewicz&Taylor [1989])

$$N_I^e(r,s) = \frac{1}{4} (1+r_I r) (1+s_I s); \quad I=1,2,3,4 \quad (3.3)$$

The in-plane displacement approximation is taken as an Allman-type interpolation (see Figure 1)

$$\begin{aligned}
\begin{pmatrix} u_1 \\ u_2 \end{pmatrix} = \mathbf{u}^h = & \sum_e \sum_{I=1}^4 N_I^e(r,s) \mathbf{u}_I \\
& + \frac{l_{JK}}{8} \sum_e \sum_{I=5}^8 NS_I^e(r,s) (\boldsymbol{\psi}_K - \boldsymbol{\psi}_J) \mathbf{n}_{JK} + \sum_e NB_9^e(r,s) \Delta \mathbf{u}_9
\end{aligned} \quad (3.4)$$

where l_{JK} and \mathbf{n}_{JK} are the length and the outward unit normal vector on the element side associated with the corner nodes J and K, i.e.

$$\mathbf{n}_{JK} = \begin{Bmatrix} n_1 \\ n_2 \end{Bmatrix} = \begin{Bmatrix} \cos \alpha_{JK} \\ \sin \alpha_{JK} \end{Bmatrix} \quad l_{JK} = ((x_{K1} - x_{J1})^2 + (x_{K2} - x_{J2})^2)^{1/2} \quad (3.5)$$

and FORTRAN-like definition of adjacent corner nodes

$$J = I - 4; \quad K = \text{mod}(I, 4) + 1 \quad (3.6)$$

In (3.4) we also employ Serendipity shape functions defined by (see Zienkiewicz&Taylor [1989])

$$NS_I^e(r,s) = \frac{1}{2} (1-r^2) (1+s_I s) ; \quad I=5,7 \quad (3.7)$$

$$NS_I^e(r,s) = \frac{1}{2} (1+r_I r) (1-s^2) ; \quad I=6,8 \quad (3.8)$$

To reflect the superior performance of the 9-node Lagrangian element over that for 8-node Serendipity element, a hierarchical bubble function interpolation is added in (3.4) where

$$NB_9^e(r,s) = (1-r^2) (1-s^2) \quad (3.9)$$

The terms in the element stiffness matrix arising from this interpolation may be eliminated at the element level by static condensation (see Wilson [1974]).

The skew-symmetric stress field is chosen constant over the element, i.e.

$$skew \tau^h = \sum_e \tau_0^e \quad (3.10)$$

We further define matrix notation

$$symm \nabla \mathbf{u}^e = \mathbf{B}_I^e \mathbf{u}_I + \mathbf{G}_I^e \psi_I \quad (3.11)$$

where \mathbf{u}_I and ψ_I are nodal values of the displacement and the rotation fields, respectively.

The \mathbf{B}_I^e matrix in (3.11) has the standard form

$$\mathbf{B}_I^e = \begin{bmatrix} N_{I,x_1}^e & 0 \\ 0 & N_{I,x_2}^e \\ N_{I,x_2}^e & N_{I,x_1}^e \end{bmatrix} ; \quad I=1,2,3,4 \quad (3.12)$$

and the part of the displacement interpolation associated with the rotation defines

$$\mathbf{G}_I^e = \frac{1}{8} \begin{bmatrix} (l_{IJ} \cos \alpha_{IJ} NS_{L,x_1}^e - l_{IK} \cos \alpha_{IK} NS_{M,x_1}^e) \\ (l_{IJ} \sin \alpha_{IJ} NS_{L,x_2}^e - l_{IK} \sin \alpha_{IK} NS_{M,x_2}^e) \\ (l_{IJ} \cos \alpha_{IJ} NS_{L,x_2}^e - l_{IK} \cos \alpha_{IK} NS_{M,x_2}^e) + (l_{IJ} \sin \alpha_{IJ} NS_{L,x_1}^e - l_{IK} \sin \alpha_{IK} NS_{M,x_1}^e) \end{bmatrix} \quad (3.13)$$

where, in (3.13) above

$$I=1,2,3,4; M=I+4; L=M-1+4 \text{ aint}(1/I); K=\text{mod}(M,4)+1; J=L-4 \quad (3.14)$$

Furthermore, we denote

$$\text{skew } \nabla \mathbf{u}^\epsilon = \mathbf{b}_I^\epsilon \mathbf{u}_I + g_I^\epsilon \psi_I \quad (3.15)$$

where

$$\mathbf{b}_I^\epsilon = \left\langle -\frac{1}{2} N_{I,x_2}^\epsilon; \frac{1}{2} N_{I,x_1}^\epsilon \right\rangle, \quad I=1,2,3,4 \quad (3.16)$$

and

$$\begin{aligned} g_I^\epsilon = & \left[-\frac{1}{16} (l_{IJ} \cos \alpha_{IJ} NS_{L,x_2}^\epsilon - l_{IK} \cos \alpha_{IK} NS_{M,x_2}^\epsilon) \right. \\ & \left. + \frac{1}{16} (l_{IJ} \sin \alpha_{IJ} NS_{L,x_1}^\epsilon - l_{IK} \sin \alpha_{IK} NS_{M,x_1}^\epsilon) - N_I^\epsilon \right]; \quad I=1,2,3,4 \end{aligned} \quad (3.17)$$

with indices J, K, L, M again defined by (3.14).

The first term in the discrete formulation (3.1) of *Problem* (M^h) gives rise to the element stiffness matrix

$$\mathbf{K}^\epsilon = \int_{\Omega^\epsilon} \left[\mathbf{B}^\epsilon \mathbf{G}^\epsilon \right]^T \mathbf{C} \left[\mathbf{B}^\epsilon \mathbf{G}^\epsilon \right] d\Omega \quad (3.18)$$

The second term in (3.1) is denoted

$$\mathbf{h}^\epsilon = \int_{\Omega^\epsilon} \langle \mathbf{b}^\epsilon; \mathbf{g}^\epsilon \rangle^T d\Omega \quad (3.19)$$

With this notation at hand, the discrete mixed-type formulation can be rewritten as

$$\begin{bmatrix} \mathbf{K}^\epsilon & \mathbf{h}^\epsilon \\ \mathbf{h}^{\epsilon T} & -\gamma^{-1} \Omega^\epsilon \end{bmatrix} \begin{Bmatrix} \mathbf{a} \\ \tau_0 \end{Bmatrix} = \begin{Bmatrix} \mathbf{f} \\ 0 \end{Bmatrix}; \quad \mathbf{a} = \begin{Bmatrix} \mathbf{u} \\ \psi \end{Bmatrix} \quad (3.20)$$

Since the skew-symmetric part of the stress is interpolated independently in each element, the corresponding part of the stiffness matrix (3.20), may be eliminated at the element level using static condensation to yield

$$\hat{\mathbf{K}}^e \mathbf{a} = \mathbf{f} ; \quad \hat{\mathbf{K}}^e = \mathbf{K}^e + \frac{\gamma}{\Omega^e} \mathbf{h}^e \mathbf{h}^{eT} \quad (3.21)$$

In a completely analogous manner we can construct an approximation for the displacement-type variational formulation. The discrete version of *Problem (D)* follows from (2.15)

Problem (D^h)

$$\begin{aligned} 0 = & \int_{\Omega^h} (\text{symm } \nabla \mathbf{v}^h) \cdot \mathbf{C} \cdot (\text{symm } \nabla \mathbf{u}^h) d\Omega \\ & + \gamma \int_{\Omega} (\text{skew } \nabla \mathbf{v}^h - \boldsymbol{\omega}^h)^T \cdot (\text{skew } \nabla \mathbf{u}^h - \boldsymbol{\psi}^h) d\Omega - \int_{\Omega} \mathbf{v}^h \cdot \mathbf{f} d\Omega \end{aligned} \quad (3.22)$$

The rotation and displacement fields are again interpolated by (3.2) and (3.4), respectively.

The first term in the displacement-type formulation (3.22) produces the same element stiffness matrix \mathbf{K}^e defined by (3.18). The second term in (3.22), however, is different. Note that using the interpolations for displacement (3.4) and rotation (3.2), this term can be directly obtained via (3.15)

$$\mathbf{P}^e = \gamma \int_{\Omega^e} \begin{Bmatrix} \mathbf{b}^e \\ \mathbf{g}^e \end{Bmatrix} \langle \mathbf{b}^e; \mathbf{g}^e \rangle d\Omega \quad (3.23)$$

Hence the matrix counterpart of (3.22) for one element in a displacement-type formulation is

$$\left[\mathbf{K}^e + \mathbf{P}^e \right] \mathbf{a} = \mathbf{f} ; \quad \mathbf{a} = \begin{Bmatrix} \mathbf{u} \\ \boldsymbol{\psi} \end{Bmatrix} \quad (3.24)$$

The parts of the element stiffness matrix \mathbf{K}^e and \mathbf{h}^e in (3.20) and (3.24) are computed using 3×3 Gaussian quadrature. The matrix \mathbf{P}^e in (3.24) is integrated by a single point Gaussian quadrature. By fully integrating \mathbf{K}^e and combining with \mathbf{P}^e or $\mathbf{h}^e \mathbf{h}^{eT} \gamma / \Omega^e$ the spurious zero energy modes are prevented; and no additional devices are needed (see, e.g. MacNeal&Harder [1988]). The 'equivalence theorem' of Malkus&Hughes [1978] may be used to show that this approach of selective reduced integration is equivalent to the mixed

formulation (3.21). The only difference in our case, however, occurs due to hierarchical interpolation of displacement field by the bubble function (see (3.4)). For selective reduced integration of the displacement-type interpolation the bubble function gives no contribution to the penalty stiffness \mathbf{P}^e , as opposed to its analog of a rank-one update ($\mathbf{h}^e \mathbf{h}^{eT} \gamma / \Omega^e$) in the mixed-type approach. This difference occurs only for skewed elements, and, as demonstrated by the numerical examples, it is of minor importance.

4. Numerical Evaluation

Several numerical examples are presented to demonstrate accuracy of the membrane element presented herein. The element is also combined with the well known DKQ plate bending element (see Batoz&Tahar [1982]) and used to solve a spherical shell with a hole, one of the problems in the set posed by MacNeal&Harder [1985]. To avoid the membrane locking and correct for element warpage, the modification suggested by Taylor [1987] and Jeteur [1987] are performed. In addition, 8-point integration rule on \mathbf{K}^e is used.

Both mixed-type (3.21) and displacement-type formulation (3.24) are evaluated. In results to follow they are denoted as M-type and D-type, respectively.

4.1 *The Patch Test*

First a patch test (see Taylor et al. [1986]) is performed on a one-element test. This will not only test the coding for our elements but can also detect any spurious modes which may exist in the elements. A skewed element (see Figure 2) is fixed with a minimum number of constraints and exposed to uniform tension. Both displacement-type and mixed-type pass the patch test.

Similar formulations with an Allman-type interpolation field (e.g., see Allman [1984] or Taylor&Simo [1985]), however, do not pass the one-element patch test. The reason is the presence of a spurious mode which occurs for constant values of nodal rotations.

4.2 *A Simple Beam: The Higher Order Patch Test*

A simple beam with a length to height aspect ratio of 10 is subjected to a pure bending state. The beam is modeled by one row of six membrane elements with drilling degrees of freedom as shown in Figure 3. No drilling degree of freedom is restrained; only a minimum number of restraints is imposed. Two load cases are considered. The first load

case is a unit couple applied at the free end and represents a higher-order patch test (see Taylor et al. [1986]). When a regular mesh is used, the solution is exact. For a distorted mesh (see Figure 3) the accuracy is still good. The second load case is, to our knowledge, a novel test. The loading is again a unit moment, but this time applied as a concentrated moment at the drilling degrees of freedom at both ends. The value of parameter γ set equal to shear modulus yields excellent results. The difference from the exact solution, for regular mesh, is due to the fact that a single concentrated moment at a drilling degree of freedom is not a consistent loading (which follows from displacement interpolation (3.4)). The results of the analysis can be compared with the beam theory exact solution of 1.5 for vertical displacement and 0.6 for end rotation.

The same analysis is repeated for the membrane element of Taylor&Simo [1985]. To prevent the occurrence of the spurious mode, besides the minimum number of restraints (see Figure 3), one drilling degree of freedom is fixed as well. The results of this analysis are also presented in Table 1. Note that, in this case, the computed rotations are wrong as dictated by the need to restrain the spurious singular rotation mode.

Formulation	Mesh	Load Case	Vert. Displ.	End Rot.
M-type	reg.	1	1.5	0.6
M-type	dist.	1	1.14185	0.57255
M-type	reg.	2	1.5	0.62070
M-type	dist.	2	1.39220	0.50612
D-type	reg.	1	1.5	0.6
D-type	dist.	1	1.14045	0.57247
D-type	reg.	2	1.5	0.62070
D-type	dist.	2	1.39200	0.49508
Taylor	reg.	1	1.5	1.2
Taylor	dist.	1	1.14195	1.10485
Taylor	reg.	2	1.5	2.18980
Taylor	dist.	2	1.39300	2.30490

4.3 A Cantilever Beam

A shear-loaded cantilever beam is selected as a test problem by many authors (e.g., see Bergan&Fellipa [1985], Allman[1988], MacNeal&Harder [1988], Hughes et al. [1989]).

The elasticity solution (e.g., see Timoshenko&Goodier [1951]) for the tip displacement is

$$u_2 = \frac{Pl^3}{3EI} + \frac{(4+5\nu)Pl}{2Eh} = 0.3553$$

for the properties selected (see Figure 4 for details, and also pages 219-220 and 254-255 of Hughes [1987]).

The finite element solution is obtained for a coarse mesh of four square elements and also for finer meshes constructed by bisection. The results obtained are compared with some of the results available in the literature. All are presented in Table 2.

Mesh	Allman	MacNeal	M-type	D-type
4×1	0.3026	0.3409	0.3445	0.3445
8×2	0.3394	-	0.3504	0.3504
16×4	0.3512	-	0.3543	0.3543
4×1*	-	0.2978	0.3066	0.3065

* irregular mesh after MacNeal&Harder [1988]

4.4 Cook's Problem

A trapezoidal membrane, suggested by Cook [1974], is another popular test problem (e.g., see Allman [1988], Bergan&Fellipa [1985], Simo et al. [1989]). Besides the shear dominated behavior (similar to the previous test), it also displays the effects of mesh distortion. The results for the tip deflection can be compared to the reference value 23.91, obtained by numerical analysis for a refined model.

Mesh	Allman	Simo	M-type	D-type
1×1	-	16.743	14.066	14.065
2×2	20.27	21.124	20.683	20.682
4×4	22.78	23.018	22.993	22.984
8×8	23.56	23.685	23.668	23.626

4.5 Hemispherical Shell with 18° Hole

The membrane presented herein is combined with a DKQ plate element (see Batoz&Thar [1982]) to construct a flat quadrilateral shell element. The performance of the shell element is evaluated on a standard test problem of a hemispherical shell with a hole (see MacNeal&Harder [1985]). It is important to establish that the proposed formulation causes no membrane locking when applied to shell analysis. The results of this analysis should be compared with the solution of 0.094 given by MacNeal&Harder [1985] and the value 0.093 suggested recently by Simo et al. [1989]. The performance of the shell element (see Table 4) is only slightly better than the one of Taylor [1987], since the difference consists only in the new membrane formulation. Even for a relatively coarse mesh, the accuracy of the element is comparable to the geometrically exact shell model of Simo et al. [1989].

Table 4. Hemispherical Shell (Fig. 6)				
Mesh	Taylor	Simo	M-type	D-type
4×4	0.086524	0.093372	0.087548	0.087528
8×8	0.094153	0.092814	0.093714	0.093701
12×12	0.093679	-	0.093587	0.093584
16×16	0.093501	0.092907	0.093488	0.093487

The analysis of this problem is repeated for different values of γ , other than $\gamma = \mu$ used to obtain the results presented in Table 4. The finite element model with the 8×8 mesh is used for this purpose. The results of the analysis are presented in Table 5. Note that the formulation is rather insensitive to the chosen value of γ . For the higher values of γ the results exhibit an asymptotic behavior. This is a consequence of enforcing the equality between the independent rotation field and skew-symmetric part of displacement gradient.

Table 5. Hemispherical Shell (Fig. 6) - Mesh 8×8		
γ / μ	M-type	D-type
0.001	0.093967	0.093853
0.05	0.093813	0.093711
1.	0.093714	0.093701
50.	0.093700	0.093700
1000.	0.093700	0.093700

5. Closure

We have presented a novel membrane element with drilling degrees of freedom based on a variational formulation which employs an independent rotation field. Both displacement-type and mixed-type formulations are considered. The element exhibits excellent accuracy characteristics for both regular and distorted meshes. The element's versatility and robustness are demonstrated on a problem where the loading is a concentrated moment directly applied at the drilling degree of freedom. When the membrane element is combined with a plate bending element, a flat shell element is formed which also performs with high accuracy.

6. References

- Allman D.J. [1984], A Compatible Triangular Element Including Vertex Rotations for Plane Elasticity Problems, *Comput. Struct.*, 19, 1-8
- Allman D.J. [1987], The Constant Strain Triangle with Drilling Rotations: A Simple Prospect for Shell Analysis, *Proceedings The Mathematics of Finite Elements and Applications*, (ed. J.R. Whiteman), Academic Press, 230-236
- Allman D.J. [1988], A Quadrilateral Finite Element Including Vertex Rotations for Plane Elasticity Problems, *Int. J. Numer. Methods Eng.*, 26, 717-739
- Bergan P.G. and C.A. Felippa [1985], A Triangular Membrane Element with Rotational Degrees of Freedom, *Comput. Methods Appl. Mech.*, 50, 25-60
- Batoz J.L. and M.B. Tahar [1982], Evaluation of a New Quadrilateral Thin Plate Bending Element, *Int. J. Numer. Methods Eng.*, 18, 1655-1677
- Carpenter N., H. Stolarski and T. Belytschko [1985], A Flat Triangular Shell Element with Improved Membrane Interpolation, *Commun. Appl. Numer. Methods*, 1, 161-168
- Cook R.D. [1974], Improved Two-Dimensional Finite Element, *ASCE J. Struct. Div.*, 100, 1851-1865
- Hughes T.J.R. [1987], *The Finite Element Method: Linear Static and Dynamic Analysis*, Prentice-Hall
- Hughes T.J.R. and F. Brezzi [1989], On Drilling Degrees of Freedom, *Comput. Methods Appl. Mech. Eng.*, 72, 105-121
- Hughes T.J.R., F. Brezzi, A. Masud and I. Harari [1989], Finite Element with Drilling Degrees of Freedom: Theory and Numerical Evaluation, preprint
- Jetteur P. [1987], Improvement of the Quadrilateral 'Jet' Shell Element for a Particular Class of Problems, IREM Internal Report 87/1, Ecole Polytechnique Federale de Laussane, Laussane
- MacNeal R.H. and R.L. Harder [1985], A Proposed Standard Set of Problems to Test Finite Element Accuracy, *J. Finite Elem. Anal. Design*, 1, 3-20
- MacNeal R.H. and R.L. Harder [1988], A Refined Four-Noded Membrane Element with Rotational Degrees of Freedom, *Comput. Struct.*, 18, 75-84

- Malkus D.S. and T.J.R. Hughes [1978], Mixed Finite Element Methods - Reduced and Selective Integration Techniques: A Unification of Concepts, *Comput. Methods Appl. Mech. Eng.*, 15, 68-81
- Reissner E. [1965], A Note on Variational Principles in Elasticity, *Int. J. Solids Struct.*, 1, 93-95
- Simo J.C., D.D. Fox and M.S. Rifai [1989], On a Stress Resultant Geometrically Exact Shell Model Part II: The Linear Theory; Computational Aspects, *Comput. Methods Appl. Mech. Eng.*, 73, 53-92
- Taylor R.L. and J.C. Simo [1985], Bending and Membrane Elements for Analysis of Thick and Thin Shells, *Proceedings NUMETA 85* (eds. J.Middelton and G.N. Pande), 587-591,
- Taylor R.L., J.C. Simo, O.C. Zienkiewicz and A.C. Chan [1986], The Patch Test: A Condition for Assessing Finite Element Convergence, *Int. J. Numer. Methods Eng.*, 22, 39-62
- Taylor R.L. [1987], Finite Element Analysis of Linear Shell Problems, *Proceedings The Mathematics of Finite Elements and Applications*, (ed. J.R. Whiteman), Academic Press, 211-223
- Timoshenko S. and J.N. Goodier [1951], *Theory of Elasticity*, McGraw-Hill
- Wilson E.L. [1974], The Static Condensation Algorithm, *Int. J. Numer. Methods Eng.*, 8, 199-203
- Zienkiewicz O.C. and R.L. Taylor [1989], *The Finite Element Method: Basic Formulation and Linear Problems*, vol I, McGraw-Hill

List of Figures

Figure 1.- A Quadrilateral Element with Drilling Degrees of Freedom

Figure 2.- The Patch Test - One-Element Test

Figure 3.- A Simple Beam

Figure 4.- Short Cantilever Beam

Figure 5.- Cook's Membrane

Figure 6.- Pinched Hemispherical Shell with an Hole

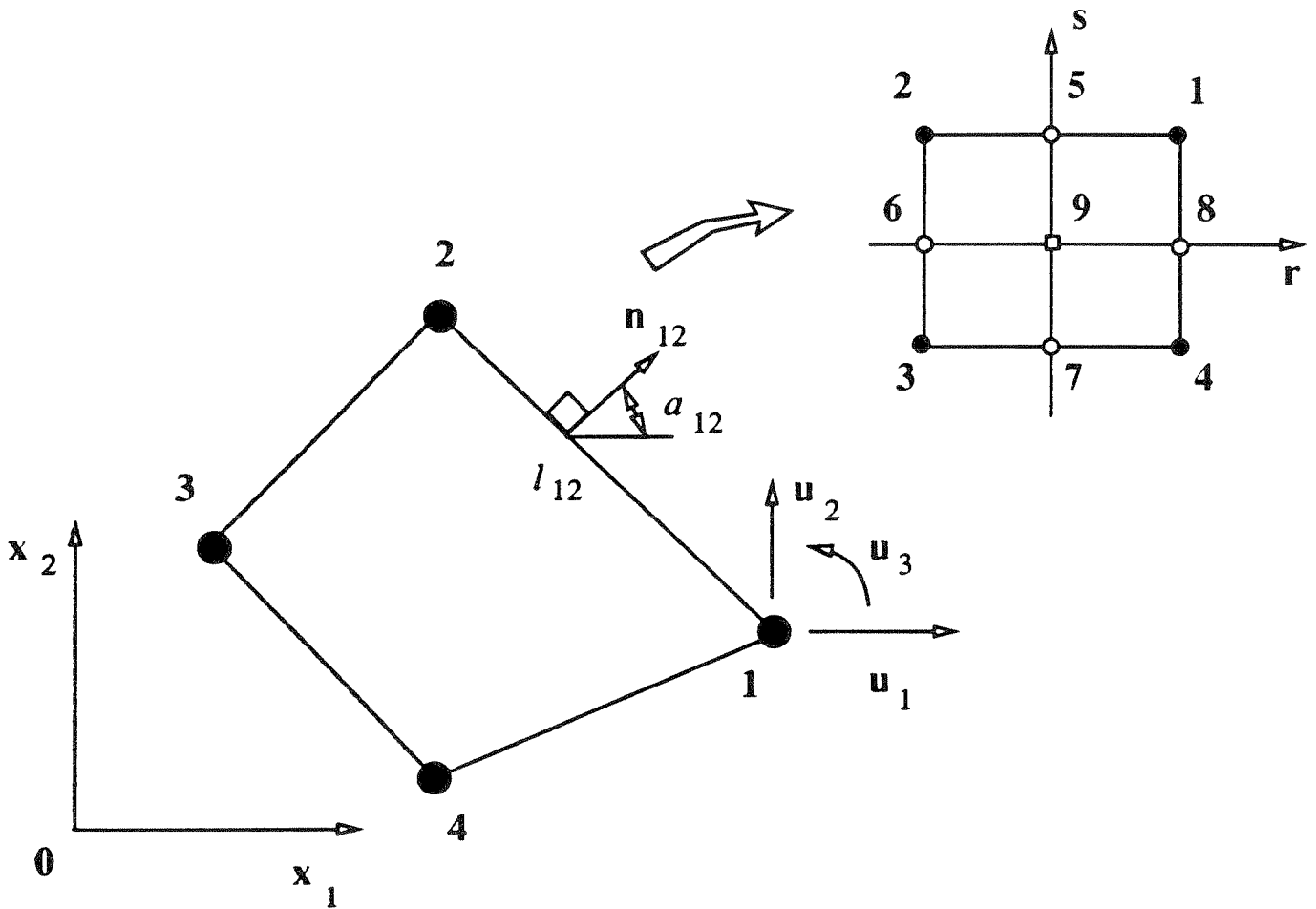


Figure 1. - A Quadrilateral Element with Drilling Degrees of Freedom

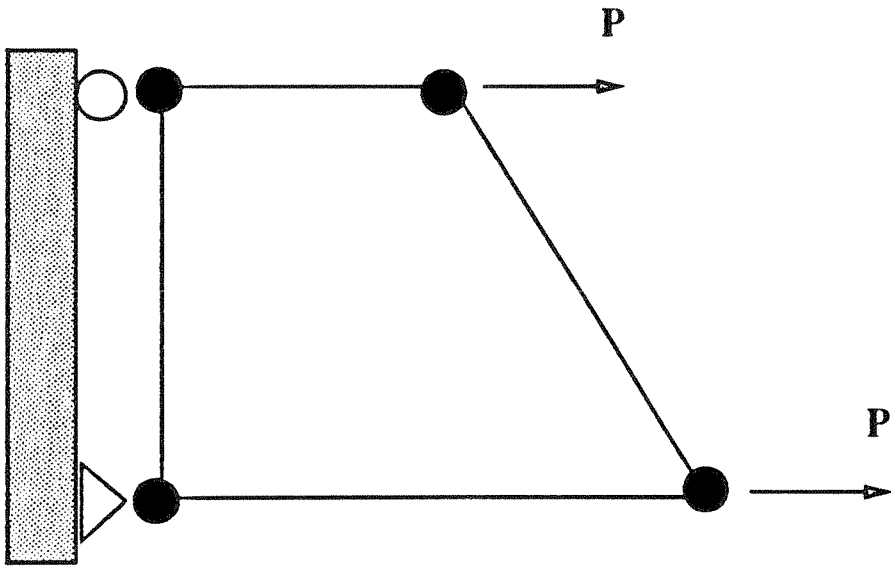
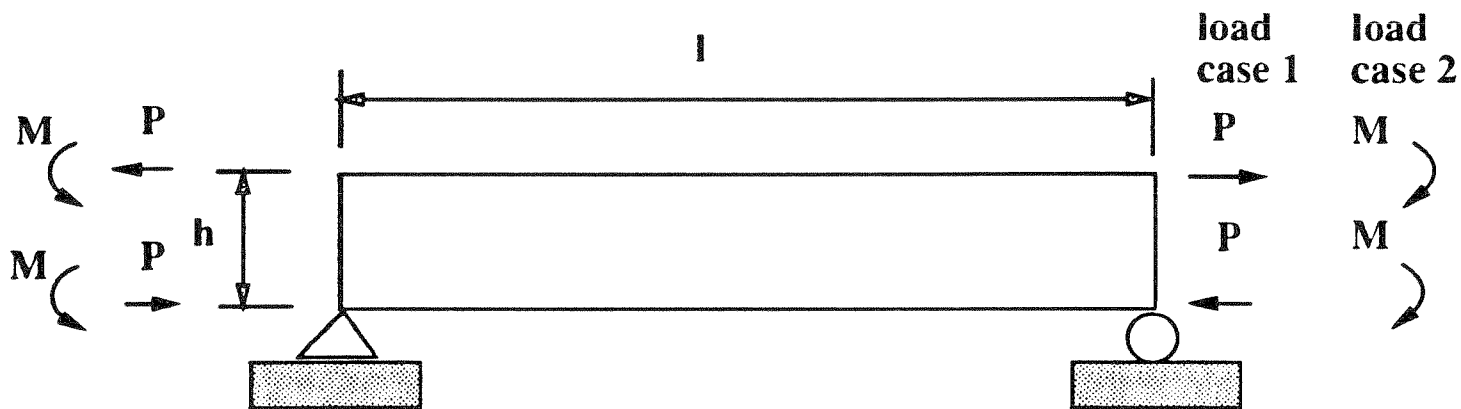
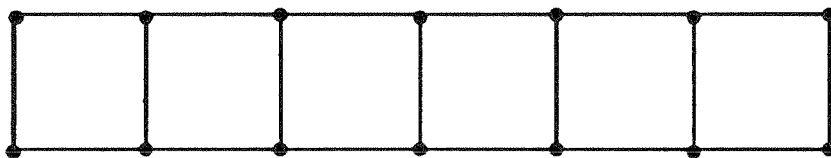


Figure 2. - The Patch Test - One-Element Test



regular mesh



$E = 100$
 $\nu = 0.3$
 $P = 1$
 $M = 0.5$
 $l = 10$
 $h = 1$

distorted mesh

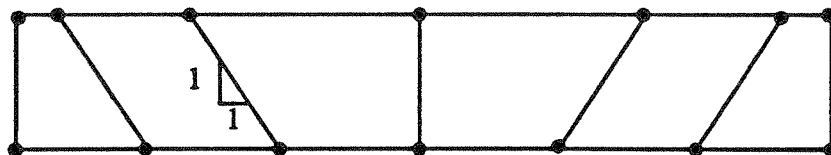
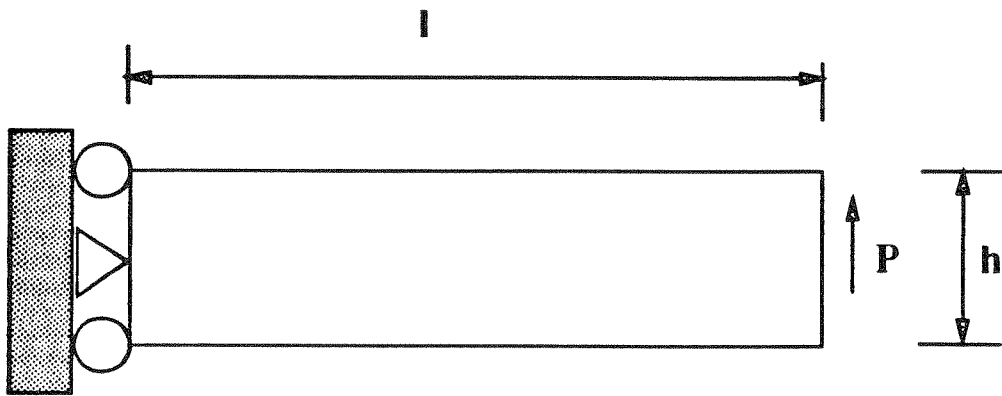
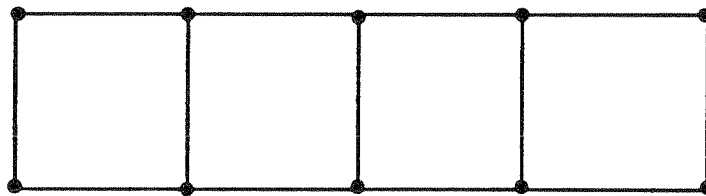


Figure 3. - A Simple Beam



regular mesh



$E = 30000$
 $\nu = 0.25$
 $P = 40$
 $l = 48$
 $h = 12$

distorted mesh

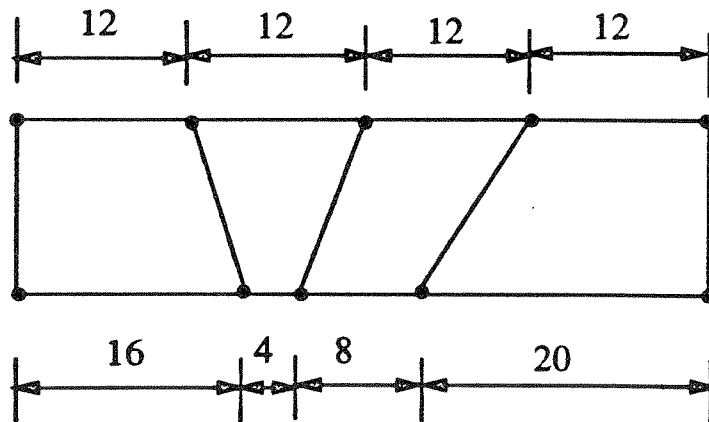
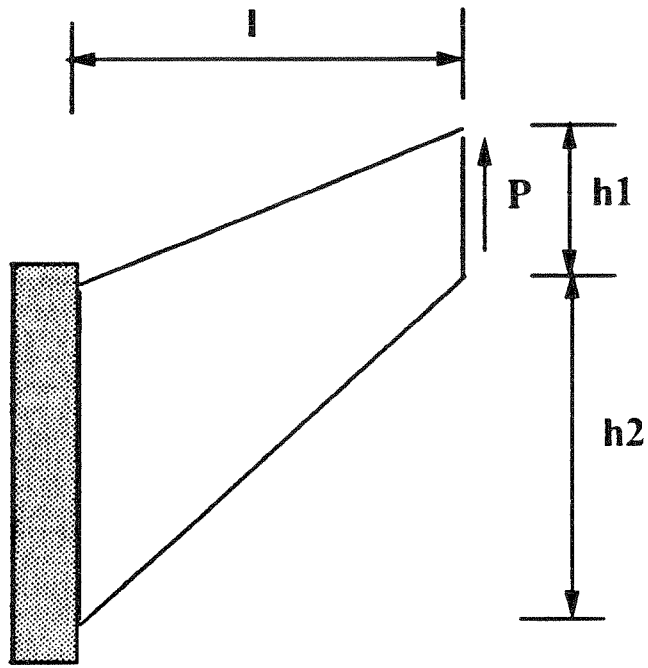


Figure 4. - Short Cantilever Beam



$E = 1$
 $\nu = 1/3$
 $P = 1$
 $l = 48$
 $h_1 = 16$
 $h_2 = 44$

FE mesh

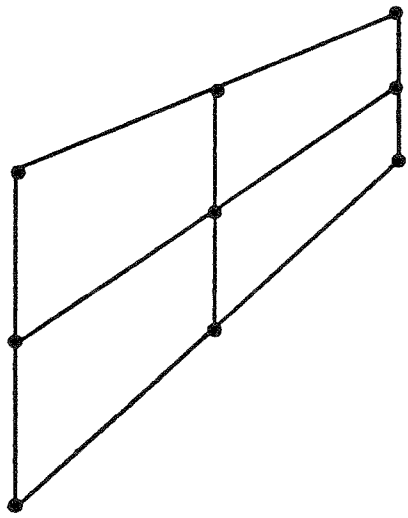


Figure 5. - Cook's Membrane

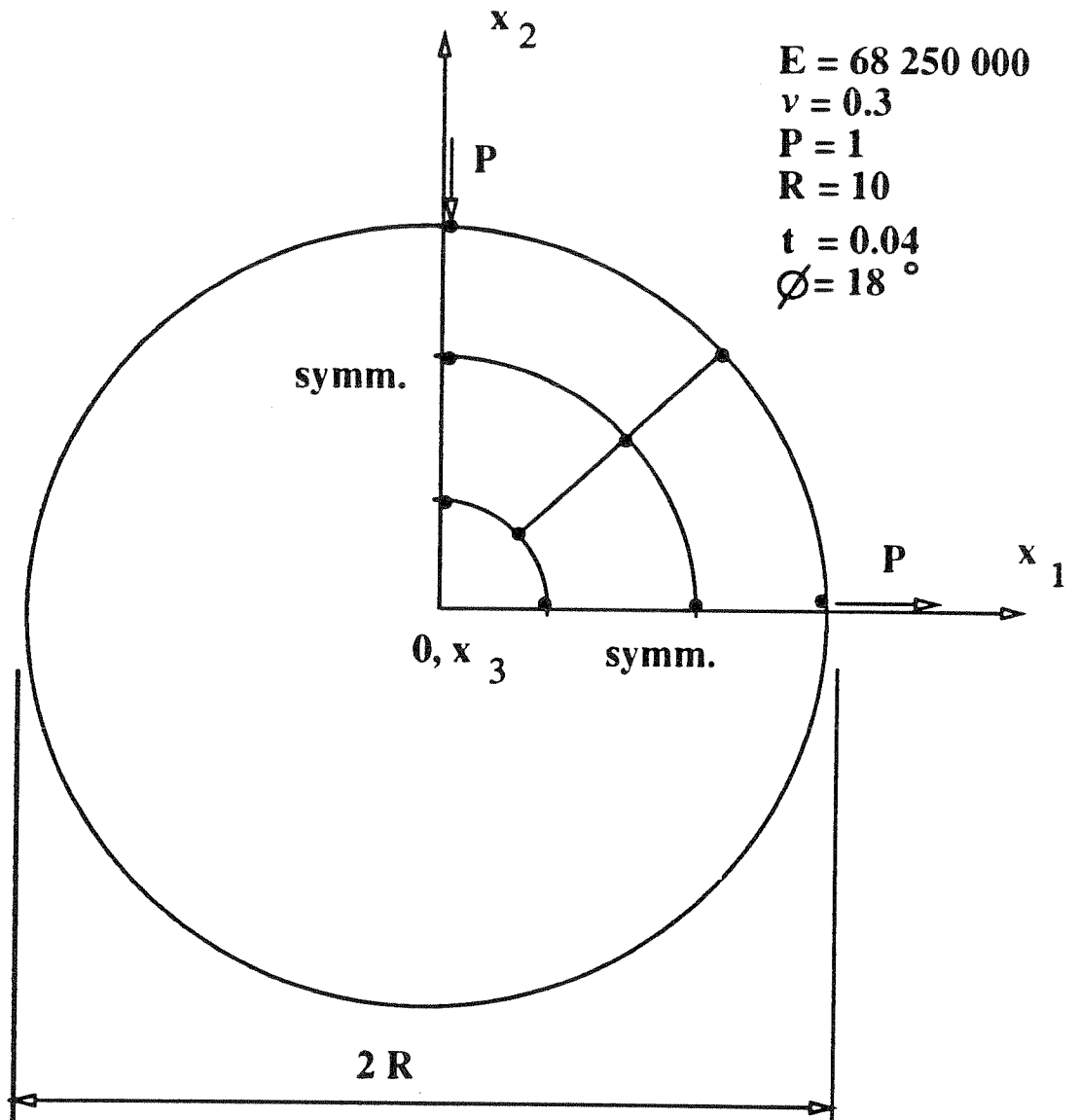


Figure 6. - Pinched Hemisphere with an Hole